Supporting Information

Charge Transport through Self-Assembled Monolayers of Monoterpenoids

Brian J. Cafferty,[1] Li Yuan,[1] Mostafa Baghbanzadeh,[1] Dmitrij Rappoport,[1] Hassan Beyzavi,[1] and George M. Whitesides[1,2,3,*]

[1]Department of Chemistry and Chemical Biology, Harvard University
12 Oxford Street, Cambridge, MA 02138, USA

[2]Kalvi Institute for Bionano Science and Technology, Harvard University,
29 Oxford Street, Cambridge, MA 02138, USA

[3]Wyss Institute for Biologically Inspired Engineering,
60 Oxford Street, Cambridge, MA 02138, USA

*Author to whom correspondence should be addressed: gwhitesides@gmwgroup.harvard.edu

Experimental

Materials. Sigma-Aldrich provided geranic acid, citronellic acid, octanoic acid, 2-octenoic acid, 3-octenoic acid, 7-octenoic acid, and 2,4,6-octatienoic acid. We synthesized 3,7-dimethyloctanoic acid and 3,7-dimethyl-2,4,6-octatrienoic acid using reported procedures.[1]

Formation of SAMs. To prepare the SAMs, we immersed Ag^{TS} substrates in a solution of 1 mM monoterpenoid, alkanoate, or alkenoate in 5 mL of anhydrous hexadecane under N_2. The samples were incubated for 3 hours. Both 3,7-dimethyl-2,4,6-octatrienoic acid and 2,4,6-octatienoic acid are not immediately soluble in hexadecane, thus, we first dissolved these molecules in a small volume of N-methyl-2-pyrrolidone (NMP) (10 µL) before adding this solution to anhydrous hexadecane. After incubation, we removed the substrates from the hexadecane solution and washed them with 3 mL of hexadecane, followed by 3 mL of THF, and dried them under a gentle stream of nitrogen. We characterized the surfaces of SAMs of 3,7-dimethyl-2,4,6-octatrienoic acid using X-ray photoelectron spectroscopy (XPS), to confirm the presence of a monolayer.

Electrical Measurements of SAMs of Isoprenoids, Alkanoates, and Alkenoates. We used our standard "1/20/1" technique (described elsewhere)[2] for electrical measurements. A fresh tip was used for each junction. Twenty scans were performed on each junction over a range of voltages from 0 to ± 0.5 V, 7-9 junctions were performed on each substrate with a minimum of two substrates used. Compounds 1-4 were tested at ± 1.0 V but after one or two unstable scans the junctions shorted.

Surface Characterization. We used angle-dependent X-ray photoelectron spectroscopy (ADXPS) and ultraviolet photoelectron spectroscopy (UPS) to characterize the SAMs of compound **1** to **9**. The ADXPS and UPS measurement were carried out by the Thermo Scientifc Nexsa XPS system with a base pressure of 10^{-7} mbar in the Center for Nanoscale Systems at Harvard University. The energy of the incident X-ray beam was at 1486.6 eV and the energy of the incident UV beam was at 40 eV. The SAMs were electrical in contact with the sample stage. We recorded the high-resolution XPS spectra of C 1*s*, O 1*s* and Ag 3*d*, at four incident angles: 90°, 75°, 60°, and 45°. The Voigt functions (a linear combination of Lorentzian (30%) and Gaussian (70 %)) were used to fit the XPS spectra with XPSpeak software. Before recording the UPS spectra, we applied 10 V to the sample stage to give secondary electrons enough kinetic energy to be recorded by the analyzer.

Statistical Analysis. We analyzed the *J*(V) data following previously reported procedures.[3] The histograms of $\log_{10}|J|$ for each bias were plotted and fitted with Gaussians to the histograms to calculate the log-mean ($\mu_{\log}$) of the values of *J* and their log standard-deviations ($\sigma_{\log}$). Figure S2 shows the histograms of $\log_{10}|J|$ at 0.5 V with Gaussian fits.

DFT Calculations. We performed density functional theory (DFT) calculations on cluster models of all four molecules of the isoprenoid series using the B3LYP hybrid exchange-correlation functional and the resolution-of-the-identity approximation for the Coulomb interaction.[4-5] The calculations employed split-valence plus polarization basis sets along with the corresponding auxiliary basis sets.[6-7] We analyzed the orbital energies and orbital shapes of the occupied π

orbitals of the monoterpenoids at their respective optimized structures. All computations used the

Turbomole quantum chemical program suite.[8]

Supplementary Figures
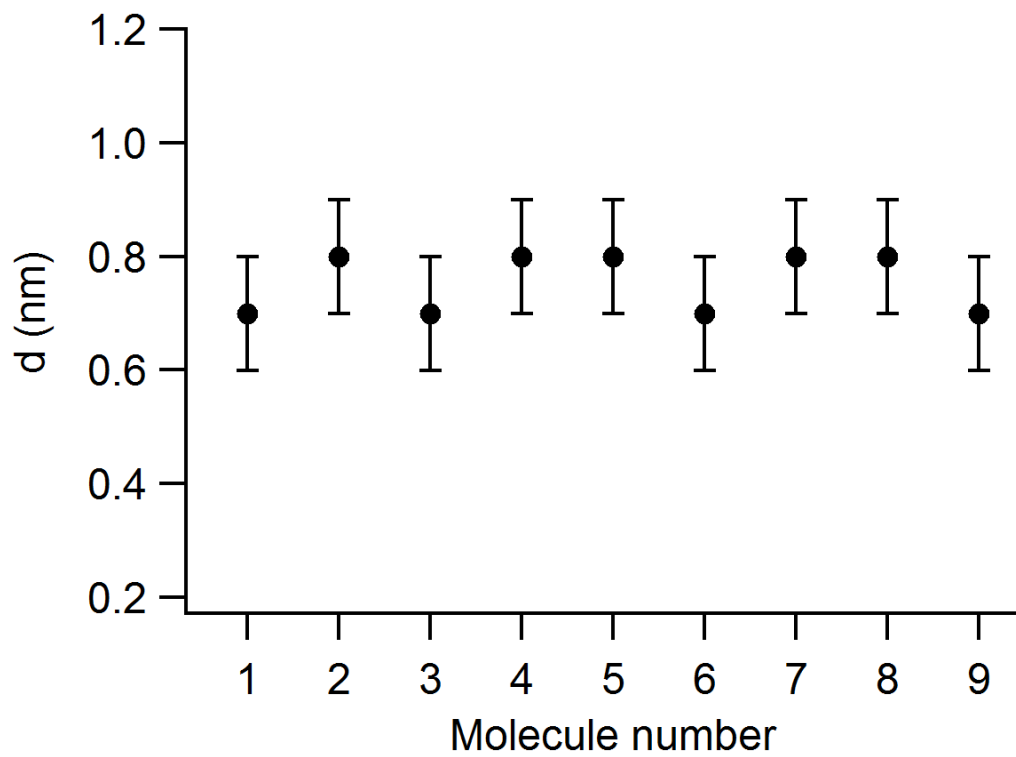
Figure S1. Plot showing the thickness of SAMs composed of each of the nine compounds determined by XPS measurements.
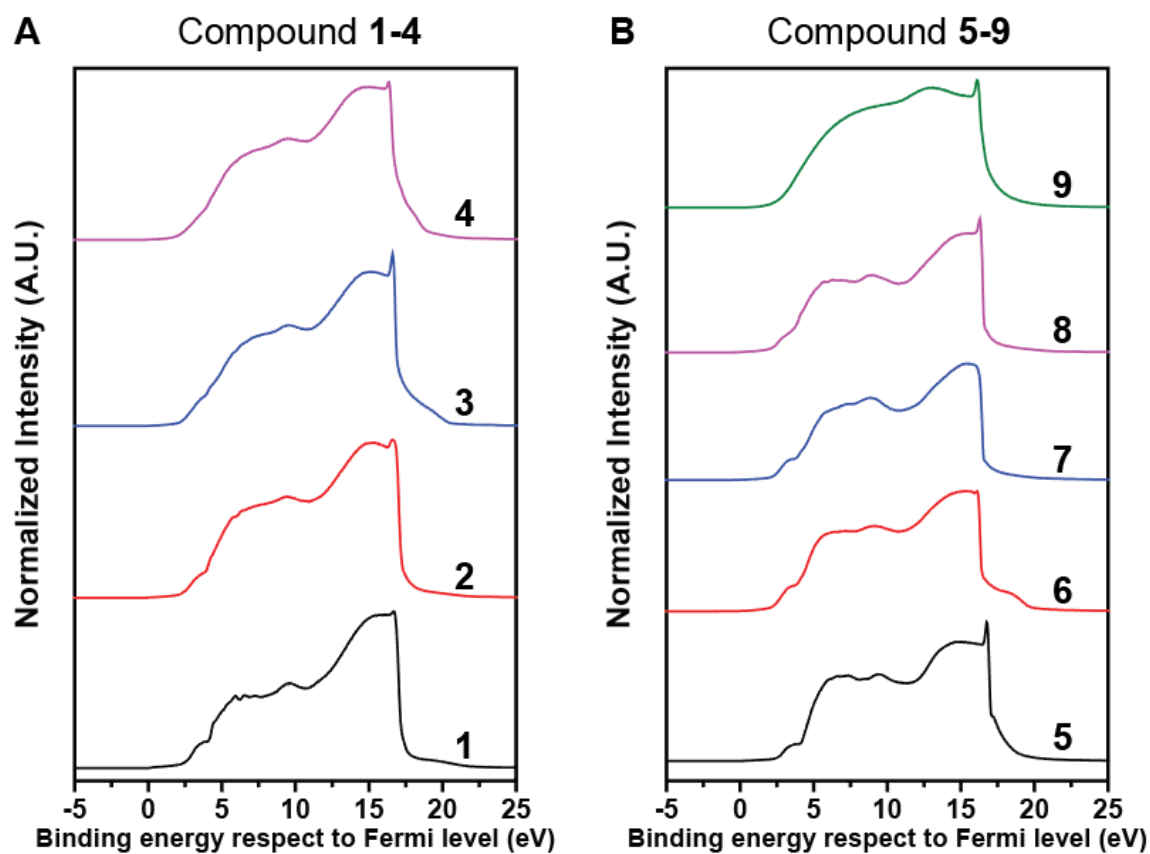
Figure S2. The UPS spectra of SAMs of compound **1-4** (**A**) and compound **5-9** (**B**). The Fermi level of the Ag electrode is at 0 eV. In the binding energy (BE) range of 0 to 5 eV with respect to the Fermi level of Ag electrode, the energy ranges from the Fermi level to HOMO-1 of the SAMs. Orbital overlapping between HOMO and HOMO-1 can be observed on SAMs of molecules **3**, **4** and **9**.

Monoterpenoids
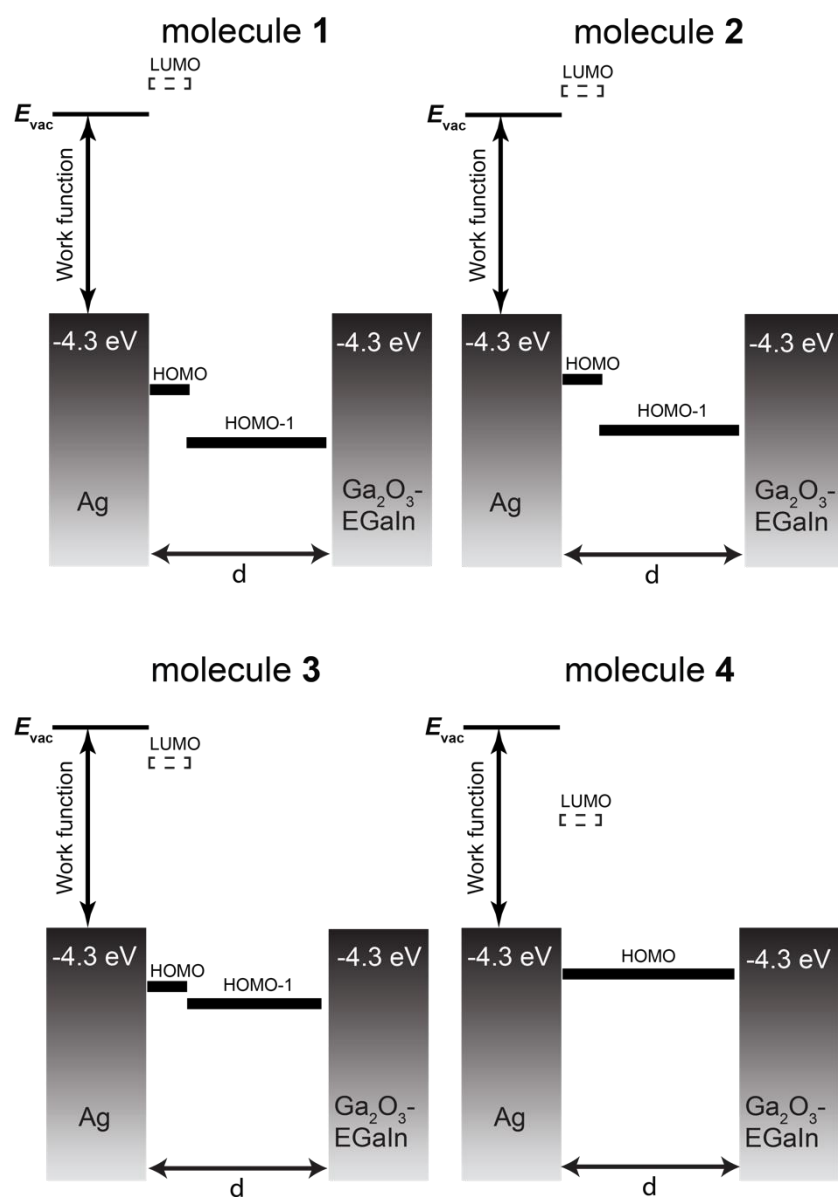
Figure S3. Energy level diagram for the four molecules of the monoterpenoid series. Energy values for the HOMO were determined by UPS, and energy levels for the LUMO were determined by DFT calculations and are relative to vacuum.
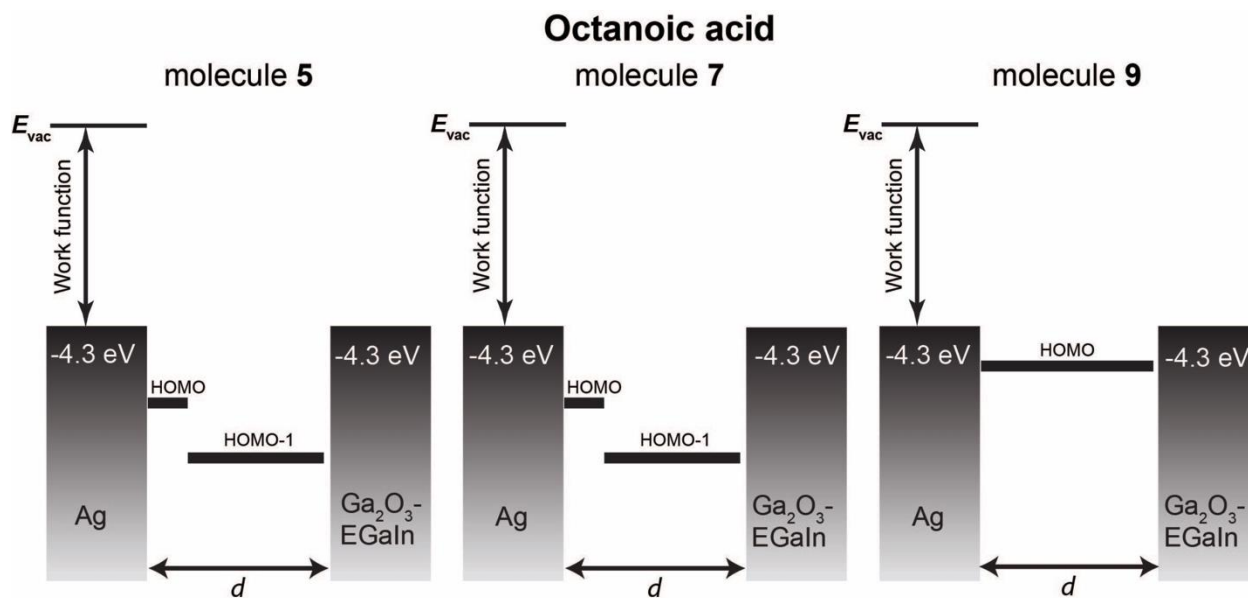
Figure S4. Energy level diagram for three molecules of the octanoic acid series. Energy values for the HOMO were determined by UPS, and energy levels for the LUMO were determined by DFT calculations and are relative to vacuum.
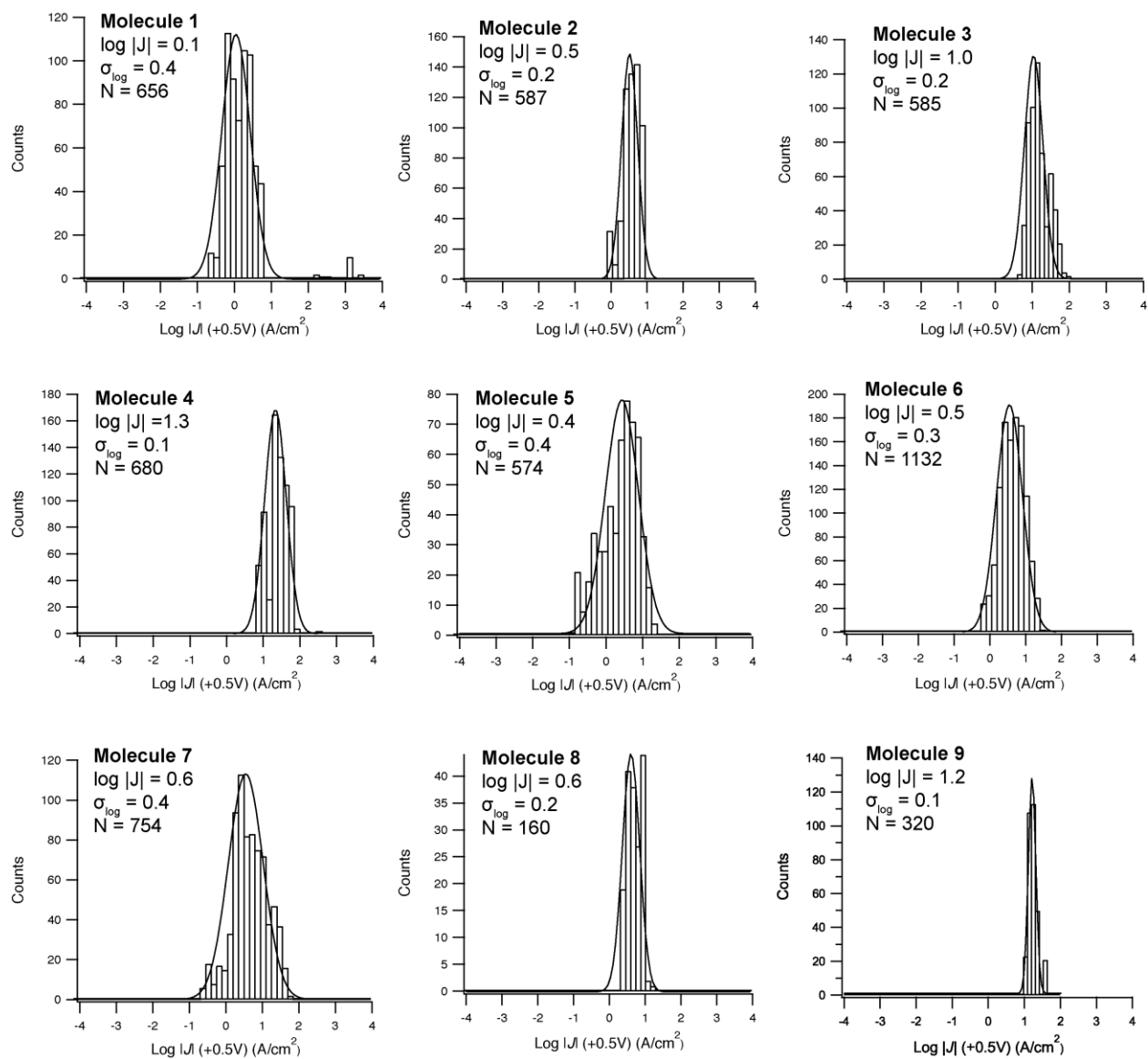
Figure S5. Histograms of the distribution of the values of log |*J*| at V = +0.5V for SAMs of monoterpenoids (molecules **1-4**) and length-matched alkanoates and alkenoates (molecules **5-9**) on Ag^TS. Solid curves represent Gaussian fits. N is the number of data points. Values of log|*J*| and $\sigma_{\log}$ are reported in each plot and were extracted from the fitting.
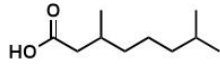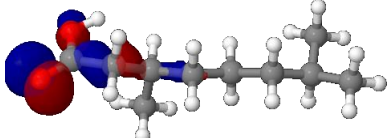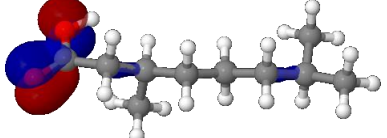
Molecule 1
9.92 Å
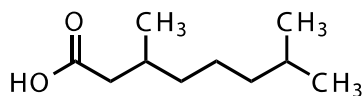
Molecule 2
9.58 Å
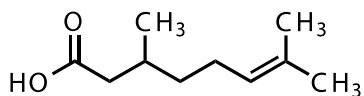
Molecule 3
9.42 Å
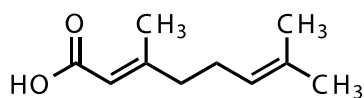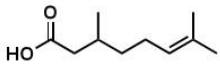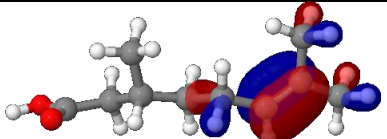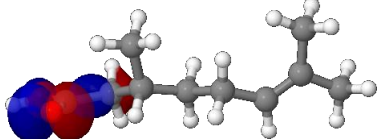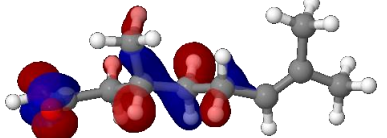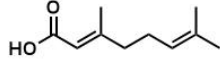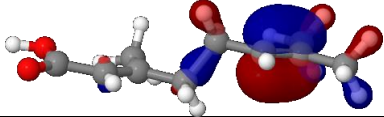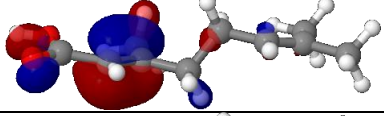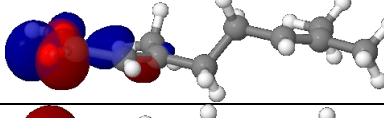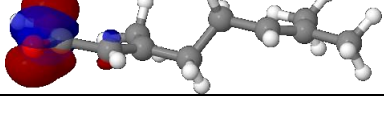
Molecule 4
9.48 Å
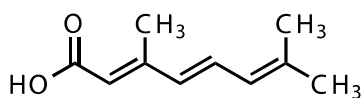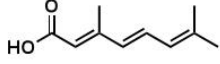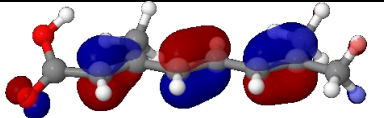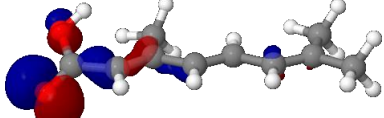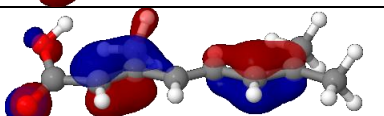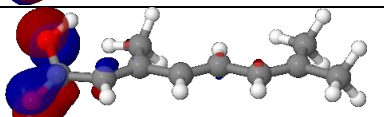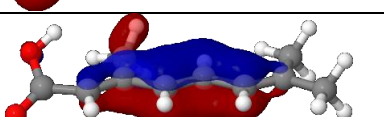
Figure S6. Lengths measured from carboxyl carbon to terminal hydrogen of optimized DFT structures. DFT calculations were based on B3LYP functional, and def2-SVP basis sets.

Table S1. Orbital energies and shapes of the highest occupied molecular orbitals (HOMO) and adjacent occupied orbitals in the monoterpenoid series examined in this study. Orbital numbers (counted in increasing order by orbital energy) are given in parentheses.

Molecule 1	Orbital Energy, eV	
HOMO (48a) COOH in-plane	–7.220	
HOMO–1 (47a) COOH out-of-plane	–8.520	

Molecule 2	Orbital Energy, eV	
HOMO (47 a) C=C π	–6.296	
HOMO–1 (46a) COOH in-plane	–7.519	
HOMO–4 (43a) COOH out-of-plane	–8.784	

	Orbital Energy, eV	
Molecule 3		
HOMO (46 a) C=C π	−6.466	
HOMO–1 (45a) C=C π	−7.119	
HOMO–2 (44a) COOH in-plane	−7.361	
HOMO–3 (43a) COOH out-of-plane	−8.565	

	Orbital Energy, eV	
Molecule 4		
HOMO (45a) C=C π	−5.926	
HOMO–1 (44a) COOH in-plane	−7.245	
HOMO–2 (43a) C=C π	−7.832	
HOMO–3 (42a) COOH out-of-plane	−8.470	
HOMO–4 (41a) C=C π	−9.222	

Table S2. List of Log|J| values at -0.5 V and $+0.5$ V and rectification ratios r⁺$_{mean}$ for molecules **1-9**.

Molecule	Log|J| at -0.5 V	Log|J| at $+0.5$ V	$r^+_{mean}(\sigma)$[a,b,c]
1	0.1 ± 0.4	0.1 ± 0.4	1.0 (1.0)
2	0.6 ± 0.2	0.5 ± 0.2	1.1 (1.0)
3	1.0 ± 0.2	1.0 ± 0.2	1.0 (1.0)
4	1.3 ± 0.1	1.3 ± 0.1	1.0 (1.0)
5	0.4 ± 0.3	0.4 ± 0.4	1.0 (1.1)
6	0.4 ± 0.4	0.5 ± 0.3	0.8 (1.0)
7	0.5 ± 0.5	0.6 ± 0.4	0.9 (1.0)
8	0.6 ± 0.1	0.6 ± 0.2	1.1 (1.0)
9	1.2 ± 0.1	1.2 ± 0.1	1.1 (1.0)

[a] r⁺$_{mean}$ is the mean rectification ratio where r⁺ = |J(+V)|/|J(-V)|.
[b] Rectification was not observed at ± 1.0 V.
[c] σ is one standard deviation of r^+_{mean}.

Supplementary References

1.   Wiley, R. H.; Imoto, E.; Houghton, R. P.; Veeravagu, P., Synthesis and Characterization of the Geometric and Structural Isomers of 3,7-Dimethyl-2,4,6-octatrienoic Acid. I. *J. Am. Chem. Soc.* **1960,** *82* (6), 1413-1416.
2.   Rothemund, P.; Morris Bowers, C.; Suo, Z.; Whitesides, G. M., Influence of the Contact Area on the Current Density across Molecular Tunneling Junctions Measured with EGaIn Top-Electrodes. *Chem. Mater.* **2017,** *30* (1), 129-137.
3.   Bowers, C. M.; Liao, K. C.; Zaba, T.; Rappoport, D.; Baghbanzadeh, M.; Breiten, B.; Krzykawska, A.; Cyganik, P.; Whitesides, G. M., Characterizing the metal-SAM interface in tunneling junctions. *ACS Nano* **2015,** *9* (2), 1471-7.
4.   Becke, A. D., Density-functional thermochemistry. III. The role of exact exchange. *The J. Chem. Phys.* **1993,** *98* (7), 5648-5652.
5.   Eichkorn, K.; Treutler, O.; Öhm, H.; Häser, M.; Ahlrichs, R., Auxiliary basis sets to approximate Coulomb potentials. *Chem. Phys. Lett.* **1995,** *240* (4), 283-290.
6.   Weigend, F.; Ahlrichs, R., Balanced basis sets of split valence, triple zeta valence and quadruple zeta valence quality for H to Rn: Design and assessment of accuracy. *Phys. Chem. Chem. Phys.* **2005,** *7* (18), 3297-305.
7.   Weigend, F., Accurate Coulomb-fitting basis sets for H to Rn. *Phys. Chem. Chem. Phys.* **2006,** *8* (9), 1057-65.
8.   Furche, F.; Ahlrichs, R.; Hättig, C.; Klopper, W.; Sierka, M.; Weigend, F., Turbomole. *Wiley Interdiscip. Rev. Comput. Mol. Sci.* **2014,** *4* (2), 91-100.